J. Biochem. **127**, 399–409 (2000)

Comparative Analysis of the Genomic Structures and Promoter Activities of Mouse Siaα2,3Galβ1,3GalNAc GalNAcα2,6-Sialyltransferase Genes (ST6GalNAc III and IV): Characterization of Their Sp1 Binding Sites[1]

Shou Takashima,[2] Nobuyuki Kurosawa,[3] Yuriko Tachida,[4] Mio Inoue,[4] and Shuichi Tsuji[5]

Molecular Glycobiology, Frontier Research Program, The Institute of Physical and Chemical Research (RIKEN), Wako, Saitama 351-0198

Received October 12, 1999; accepted December 9, 1999

The genomic organization of the genes encoding the mouse *N*-acetylgalactosamine α2,6-sialyltransferase specific for Siaα2,3Galβ1,3GalNAc (ST6GalNAc III and IV) has been determined. The ST6GalNAc III gene spans over 120 kilobases of genomic DNA with 5 exons; on the other hand, the ST6GalNAc IV gene spans over 12 kilobases of genomic DNA with 6 exons. But the exon–intron boundaries of these genes are very similar. The 5′-flanking regions of these genes do not contain a TATA- or CAAT-box but have three putative Sp1 binding sites for each promoter. Transient transfection experiments demonstrated functional promoter activity in an ST6GalNAc III–expressing cell line, P19, for the ST6GalNAc III promoter, and in an ST6GalNAc IV–expressing cell line, NIH3T3, for the ST6GalNAc IV promoter. Mobility shift assaying and mutational analysis of the promoter region indicated that two of the three Sp1 binding sites are involved in the transcriptional regulation of the ST6GalNAc III gene in P19 cells, while all three Sp1 binding sites are involved in the transcriptional regulation of the ST6GalNAc IV gene in NIH3T3 cells.

Key words: GalNAc α2,6-sialyltransferase, GD1α synthase, genomic structure, molecular cloning, sialyltransferase.

The NeuAcα2,6GalNAc-structure is known to be a common feature of *O*-linked oligosaccharides and α-series gangliosides. The transfer of sialic acid to *N*-acetylgalactosamine (GalNAc) from CMP–sialic acid is catalyzed by a family of sialyltransferases, GalNAc α2,6-sialyltransferases (ST6GalNAc-family) (*3*, *4*). So far, the cDNA cloning of five members of the α2,6-sialyltransferase family (ST6GalNAc I–V) has been reported (*5–12*). Mouse ST6GalNAc I and II exhibit high amino acid sequence homology in their active domains and transfer sialic acid to α-linked GalNAc (GalNAcα1,*O*-Ser/Thr), but not to β-linked GalNAc. ST6GalNAc I and II exhibit the broadest substrate specificity, transferring CMP-NeuAc with an α2,6-linkage to the GalNAc residues of GalNAc-*O*-Ser/Thr, Galβ1,3GalNAc-*O*-Ser/Thr, and NeuAcα2,3Galβ1,3GalNAc-*O*-Ser/Thr (*5*). Both genes are expressed in secretory organs, such as the submaxillary and mammary glands, so the enzymes are considered to be involved in the biosynthesis of the *O*-glycans of mucin. On the other hand, ST6GalNAc III, IV, and V exhibit the most restricted substrate specificities, only utilizing the NeuAcα2,3Galβ1,3GalNAc-sequence as an acceptor, however, there are some differences in their substrate preferences. ST6GalNAc III can transfer sialic acid to both NeuAcα2,3Galβ1,3GalNAc-*O*-Ser/Thr and ganglioside GM1b. ST6GalNAc IV exhibits strong activity toward NeuAcα2,3Galβ1,3GalNAc and *O*-glycans (*9*). On the other hand, ST6GalNAc V exhibits strong activity toward GM1b and very weak activities toward *O*-glycans. At present, ST6GalNAc V is considered to be the most probable candidate for GD1α synthase (*12*). GD1α has been assumed to be a molecular component involved in a variety of important biological processes including the metastasis of highly virulent lymphomas and motor learning as worked out by Purkinje cells

[1] This work was supported by the following grants: Grants-in-Aid for Scientific Research on Priority Areas, Nos. 10152263 and 10178104, and for Scientific Research, B 11480216, from the Ministry of Education, Science, Sports and Culture of Japan. The nucleotide sequences reported in this paper have been submitted to the GenBank™/EBI Data Bank under accession numbers Y11342-6 (ST6GalNAc III gene) and Y19053-7 (ST6GalNAc IV gene).

[2] Present addresses: Laboratory for Neural Regeneration, Brain Science Institute, The Institute of Physical and Chemical Research (RIKEN), Wako, Saitama 351-0198; [3] Department of Biochemistry, Nagoya University School of Medicine, 65 Tsurumai-cho, Showa-ku, Nagoya 466-8550; [4] Laboratory for Protein Research, Genomic Science Center, The Institute of Physical and Chemical Research (RIKEN), Wako, Saitama 351-0198

[5] To whom correspondence should be addressed. Tel/Fax: +81-463-85-5301, E-mail: stsuji02@yhb.att.ne.jp

[6] Takashima, S., Tachida, Y., and Tsuji, S., unpublished observation.

Abbreviations: The nomenclature for gangliosides follows the system of Svennerholm (*1*). The abbreviated nomenclature for cloned sialyltransferases follows the system of Tsuji *et al.* (*2*). ST6GalNAc I, GalNAc α2,6-sialyltransferase (EC 2.4.99.3); ST6GalNAc II, Galβ1,3GalNAc GalNAc α2,6-sialyltransferase; ST6GalNAc III-V, Siaβ2,3Galβ1,3GalNAc GalNAcα2,6-sialyltransferase (EC 2.4.99.7); Sia, sialic acid; NeuAc, *N*-acetylneuraminic acid; CMP-NeuAc, cytidine 5′-monophospho-*N*-acetylneuraminic acid; PCR, polymerase chain reaction; kb, kilobases; bp, base pairs.

(*13*, *14*). The expression of GD1α is highest in the embryonic brain, with a lower level in adults.

Besides substrate preferences, the mRNA expression levels of ST6GalNAc III and IV are dramatically different, although their expression patterns are similar but not identical (*9*). The expression levels of ST6GalNAc IV is much higher than that of III in almost all tissues, suggesting that the promoter of ST6GalNAc IV is stronger than that of III. Thus, it is necessary to elucidate the different regulatory mechanisms for the gene expression of ST6GalNAc III and IV. In the present study, we have cloned mouse ST6GalNAc III and IV genomic DNAs and characterized their promoters.

MATERIALS AND METHODS

Isolation of Mouse ST6GalNAc III and IV Genomic Clones—An NIH3T3 genomic cosmid library (*15*) was screened with mouse ST6GalNAc III cDNA (*9*) as a probe. A C57BL/6 gemonic cosmid library was constructed as described previously (*8*) using a pWE15 cosmid vector kit (Stratagene) and *Eschelichia coli* XL1-Blue as a host, and screened with mouse ST6GalNAc IV cDNA (*9*) as a probe. Cosmid DNAs from the positive bacterial colonies were isolated and then subjected to restriction analysis. The locations of the exons of the sialyltransferase genes were determined by PCR with specific oligonucleotide primers or by hybridization. For general DNA manipulation, *E. coli* JM109 and MV1184 were used as hosts for cloning vectors.

PCR Amplification of the 5′-cDNA End (RACE)—The primers used in this paper are listed in Table I. Amplification of the 5′-end of mouse ST6GalNAc III cDNA was performed as described previously (*5*, *9*). cDNA was synthesized by the reverse transcription (Superscript II, GIBCO BRL) of 5 μg of mouse brain poly(A)$^+$RNA and NB41A3 cell poly(A)$^+$RNA using primer RT-181. The cDNA was A-tailed with 0.6 unit of terminal deoxynucleotidyltransferase (Boehringer Mannheim, Germany) using 0.05 mM dATP. Two consecutive PCRs were performed with two nested sets of primers. For pair 1, the forward primer was *Not*I-d(T)$_{18}$ (Pharmacia, Sweden) and the reverse primer was RT-181. For pair 2, the forward primer was as above but without the T-tail [*Not*I-d(T)$_0$], and the reverse primer was RT-91. The cDNA was amplified through 35 cycles of a step program (94°C, 30 s; 55°C, 30 s; 72°C, 40 s). The amplified products were blunt-ended, kinated, digested with *Eco*RI, and then subcloned into the *Eco*RI/*Sma*I site of pUC119. pE91 was constructed by subcloning the 0.5 kb PCR product amplified with RT-91 and a reverse sequencing primer (M13 primer RV, Takara, Kyoto), into the *Eco*RI/*Sma*I site of pUC119, followed by kination and *Eco*RI digestion. Dideoxy chain-termination sequencing of RACE clones was carried out on a 6% sequencing gel along with a corresponding control sequence ladder. Amplification of the 5′-end of mouse ST6GalNAc IV cDNA was performed using a 5′-full RACE core set (Takara) and 1 μg of mouse brain poly(A)$^+$RNA according to the manufacturer's instructions. For cDNA synthesis, the ST6GalNAc IV cDNA–specific primer, R1-7-, was used, and the cDNA was self-ligated. Then two consecutive PCRs were performed with the above self-ligated cDNA as a template using the first primer set, R1-5+ and R1-3-; the second PCR was performed with 1 μl of the above reaction mixture as a template using the second primer set, R1-6+ and R1-2-. The amplified products were blunt-ended and cloned into the *Eco*RV site of pBluescript II SK(+), and then sequenced.

PCR Amplification of the 3′-cDNA End (RACE)—Amplification of the 3′-end of mouse ST6GalNAc IV cDNA was performed using a 3′-full RACE core set (Takara) and 1 μg of mouse brain poly(A)$^+$RNA according to the manufacturer's instructions. For PCR amplification, the ST6GalNAc IV cDNA–specific primers, R1-13+, R1-14+, and R1-10+, were used. The amplified products were blunt-ended and cloned into the *Eco*RV site of pBluescript II SK(+), and then sequenced.

Primer Extension Analysis—The ST6GalNAc IV cDNA–specific primer, R1-1-, was end-labeled with [γ-^{32}P]ATP using T4 polynucleotide kinase. The radiolabeled primer was hybridized with 5 μg of poly(A)$^+$ RNAs prepared from mouse brain or colon, or 5 μg of yeast tRNA as a control as

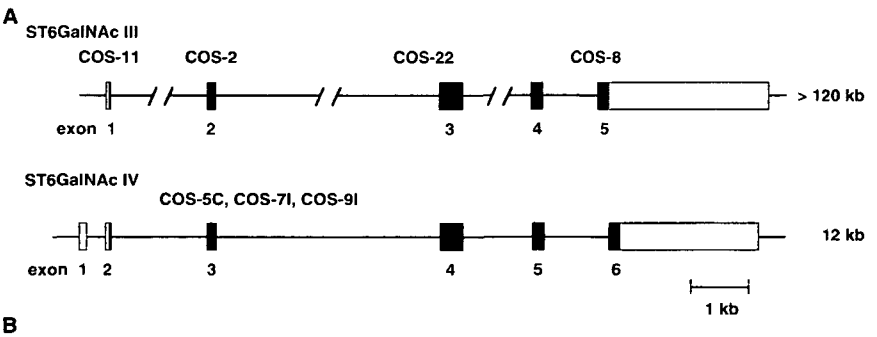

B

ST6GalNAc III		Homology (%)	ST6GalNAc IV	
exon No.	number of residues		number of residues	exon No.
		—	—	1
1	6	—	4	2
2	65	36	62	3
3	137	52	138	4
4	36	65	36	5
5	61	66	62	6

Fig. 1. **Comparison of the genomic structures of the ST6GalNAc III and IV genes.** (A) Exon/intron structures of the ST6GalNAc III and IV genes. For the ST6GalNAc III gene, four independent genomic clones (COS-11, COS-2, COS-22, and COS-8) were isolated from a cosmid library. For the ST6GalNAc IV gene, three overlapping genomic clones (COS-5C, COS-7I, and COS-9I) were isolated from a cosmid library. The protein coding regions, and the 5′- and 3′-untranslated regions are shown by filled rectangles and open rectangles, respectively. The intronic sequences are shown by the solid lines between the exons. (B) Comparison of the deduced amino acid sequences of the exons of the ST6GalNAc III gene with those of the corresponding exons of the ST6GalNAc IV gene.

to extension specificity, and then extended with Superscript II reverse transcriptase (GIBCO BRL) as described previously (*16*). The primer extension products were separated on a 6% sequencing gel along with a corresponding control sequence ladder.

Analysis of Promoter Activity—A 2.0 kb *Eco*RI fragment containing mouse ST6GalNAc III exon 1 was isolated from the COS-11 clone (Fig. 1A) and then subcloned into the pBluescript SK(+) plasmid. The resultant plasmid, designated as pEX1-E2.0, was used for construction of reporter plasmids. A ST6GalNAc III–luciferase reporter plasmid, pB8-471, was constructed by subcloning a 471 bp *Xho*I/*Nco*I fragment from pEX1-E2.0 into the *Xho*I/*Nco*I sites of pPicaGene-Basic vector II (pPGBII; Toyo-ink, Tokyo). pB8-189 was constructed by subcloning a 189 bp *Hin*dIII/*Nco*I-digested PCR fragment into pPGBII. PCR was performed using the primers B8-*Hin*dIII and RT91, with pEX1-E2.0 as the template. pB8-7.2K was constructed by subcloning a 7.0 kb *Sac*I/*Bgl*II fragment from the COS-11 clone into the *Sac*I/*Bgl*II sites of pB8-471. pB8-1650 was constructed by subcloning a 1650 bp *Sma*I/*Nco*I fragment into pPGBII.

ST6GalNAc IV–luciferase reporter plasmids were constructed as follows. pR1-1232 was constructed by subcloning a 1232 bp *Hin*dIII/*Nco*I-digested PCR fragment into pPGBII. PCR was performed using the primers R1-*Hin*dIII(A) and R1-2-, with the COS-7I clone (Fig. 1A) as the template. pR1-1022 was constructed by subcloning a 1022 bp *Hin*dIII/*Nco*I-digested PCR fragment into pPGBII. PCR was performed using the primers R1-*Hin*dIII(B) and R1-2-, with the COS-7I clone as the template. pR1-819 was constructed by subcloning an 819 bp *Xho*I/*Nco*I-digested PCR fragment into pPGBII. PCR was performed using the primers R1-*Xho*I and R1-2-, with the COS-7I clone as the template. pR1-262 was constructed by subcloning a 262 bp

TABLE I. **Primers used in this study.**

Primer	Sequence	Strand	Position
ST6GalNAc III			
RT-91	5′-CTTGAGGATGCAGGCCATGGCGCTATG-3′	Antisense	63 to 89
RT-181	5′-TTAGGCTGTCCAAAGCAGTTCAGG-3′	Antisense	179 to 202
*Not*I-d(T)$_{18}$	5′-AACTGGAAGAATTCGCGGCCGCAGGAA(T)18-3′		
*Not*I-d(T)$_0$	5′-AACTGGAAGAATTCGCGGCCGCAGGAA-3′		
M13 primer RV	5′-CAGGAAACAGCTATGAC-3′		
B8-*Hin*dIII	5′-GCAAGCAAGCTTAGTTGCGGGCTGCACG-3′ (the *Hin*dIII linker was underlined)	Sense	−118 to −102
B8-GS1+	5′-GTGACTAGGGGCGGGGCCTCGTGTGGCGCC-3′	Sense	−94 to −65
B8-GS1−	5′-GCTGGCGCCACACGAGGCCCCGCCCCTAGT-3′	Antisense	−91 to − 62
B8-GS2+	5′-TCGTGTGGCGCCAGCCAGTGGCGGGGCT-3′	Sense	−76 to −49
B8-GS2−	5′-CCGAGCCCCGCCACTGGCTGGCGCCACA-3′	Antiense	−73 to −46
B8-GS3+	5′-GGCTCGGGGGTGGGGGCCTGAGCGCGC-3′	Sense	−52 to −27
B8-GS3-	5′-CGTGCGCGCTCAGGCCCCCACCCCCGA-3′	Antisense	−49 to −24
B8-Sp1A	5′-CGCCACACGAGGCCCAGATCTTAGTCACGTGCCCTC-3′ (the *Bgl*II linker is underlined),	Antisense	−102 to −67
B8-Sp1B	5′-GCCCCACCCCCGAGCGGATCCACTGGCTGGCGCC-3′ (the *Bam*HI linker is underlined),	Antisense	−70 to −37
B8-Sp1C	5′-GTGCGCGCTCAGGCCGAATTCCCGAGCCCCGCCAC-3′ (the *Eco*RI linker is underlined)	Antisense	−59 to −25
ST6GalNAc IV			
R1-1−	5′-GCTGCTCGGAGCTCCATGTC-3′	Antisense	81 to 100
R1-2−	5′-GGGCCTTCATGCTGTCTCTG-3′	Antisense	219 to 238
R1-3−	5′-AGGCAGGTTGCCAGGCAGAG-3′	Antisense	322 to 341
R1-5+	5′-TTGAGGAGGACGTGGGCCAG-3′	Sense	471 to 490
R1-6+	5′-GCCTGCAAGTGTACACCTTC-3′	Sense	761 to 780
R1-7−	5′-CTGACCATCCCGTAGACCAC-3′	Antisense	913 to 932
R1-10+	5′-GGTGGGATCTAGACTACTCC-3′	Sense	3469 to 3488
R1-13+	5′-TTAAGTGACCTTTGCCCTGG-3′	Sense	1401 to 1420
R1-14+	5′-TCTCTGTGGTAACGGATGTG-3′	Sense	1645 to 1664
R1-*Hin*dIII(A)	5′-AAGCTTGAATTCCAGTACTTGGGAGGCAGA-3′ (the *Hin*dIII linker is underlined)	Sense	−651 to −628
R1-*Hin*dIII(B)	5′-GTTTGAAGCTTGCCTGAAAAAT-3′ (the *Hin*dIII linker is underlined)	Sense	−451 to −430
R1-*Xho*I	5′-CTCAATTCTCGAGGGCCAGTAGC-3′ (the *Xho*I linker is underlined)	Sense	−251 to −229
R1-*Mlu*I	5′-GACCTTGAGCCGAACGCGTCTCCTCTTT-3′ (the *Mlu*I linker is underlined)	Sense	Located at the first intron
R1-GS1+	5′-CTAGACAGGCCCCGCCCTCGACGT-3′	Sense	−162 to −139
R1-GS1−	5′-CGACGTCGAGGGCGGGGCCTGTCT-3′	Antisense	−160 to −137
R1-GS2+	5′-CGTCGAGACCTCGCCCCCCAGCCC-3′	Sense	−141 to −118
R1-GS2−	5′-CCGGGCTGGGGGGGCGAGGTCTCGA-3′	Antisense	−139 to −116
R1-GS3+	5′-GCGCAGGCCCCGCCCCCTGAGCGC-3′	Sense	−78 to −55
R1-GS3−	5′-TTGCGCTCAGGGGGCGGGGCCTGC-3′	Antisense	−76 to −53
R1-Sp1A′	5′-AACTAGACAGGCCACGCGTTCGACGTCGAGAC-3′ (the *Mlu*I linker is underlined)	Sense	−164 to −133
R1-Sp1B′	5′-TCGACGTCGAGACTTCGAACCCCAGCCCGGAG-3′ (the *Nsp*V linker is underlined)	Sense	−145 to −114
R1-Sp1C′	5′-CGCTGCGCAGGCCCAGATCTCTGAGCGCAAAGC-3′ (the *Bgl*II linker is underlined)	Sense	−82 to −50

*Mlu*I/*Nco*I-digested PCR fragment into pPGBII. PCR was performed using the primers R1-*Mlu*I and R1-2-, with the COS-7I clone as the template. pR1-8.6K was constructed by subcloning a 8.1 kb *Sac*I fragment from the COS-7I clone into the *Sac*I site of pR1-1232. pR1-5.1K was constructed by deleting a 3.5 kb *Kpn*I/*Xho*I fragment from pR1-8.6K, followed by blunt-ending and self-ligation. The resultant chimeric constructs were transfected into P19 cells (embryonal carcinoma) and NIH3T3 cells (fibroblast) for analysis of the ST6GalNAc III and IV promoter activities, respectively. The cell lines were obtained from American Type Culture Collection (ATCC) and RIKEN Cell Bank. Cells were seeded at 1×10^5 cells per 60-mm diameter dish in Dulbecco's Modified Eagle's Medium–10% fetal calf serum 24 h prior to transfection. Each luciferase plasmid (5 μg) and a pSRβ-Gal plasmid (0.5 μg), which served as an internal control as to transfection efficiency, were transfected into the cells with LipofectAMINE (GIBCO BRL). After 48 h transfection, the cells were washed three times with PBS and then lysed with cell lysis buffer (PGC-51; Toyo-ink). Luciferase activity was measured with a PicaGene Luciferase Assay System (Toyo-ink) and a Luminescencer AB-2000 (ATTO, Tokyo). Light activity measurements were made in triplicate, averaged, and then normalized as to β-galactosidase activity in order to correct for transfection efficiency. β-Galactosidase activity was measured with a Luminescent β-Galactosidase Detection Kit II (Clontech).

Mobility Shift Assay—For the ST6GalNAc III promoter, a DNA fragment comprising nucleotides –94 to 74 was prepared from pB8-189 by digestion with *Pma*CI and *Nco*I, and then end-labeled with [α-^{32}P]dCTP using Klenow polymerase. Binding assays were performed as described previously (*16*). The annealed pairs of synthetic DNA fragments, B8-GS1+ and B8-GS1-, B8-GS2+ and B8-GS2-, and B8-GS3+ and B8-GS3-, were used as competitors.

For the ST6GalNAc IV promoter, a DNA fragment comprising nucleotides –238 to 25 was prepared from pR1-819 by digestion with *Xho*I and *Eco*52I, and then end-labeled with [α-^{32}P]dCTP using Klenow polymerase. Binding assays were performed as described previously (*16*). The annealed pairs of synthetic DNA fragments, R1-GS1+ and R1-GS1-, R1-GS2+, and R1-GS2-, and R1-GS3+ and R1GS3-, were used as competitors.

Site-Directed Mutagenesis of the Sp1 Binding Sites—For the ST6GalNAc III promoter, Sp1 binding site-replaced mutants, pB8-189(Sp1A), pB8-189(Sp1B), pB8-189(Sp1C), and pB8-189(Sp1AC), were constructed as follows. A 880 bp *Sph*I–*Hin*dIII fragment of pB8-189 was subcloned into pKF19k (Takara), and then subjected to site-directed mutagenesis using mutagenic primers, *i.e.* B8-Sp1X for Sp1 binding site X (X = A, B, and C), with a Mutan-Super Express Km kit (Takara). From these mutagenized plasmids, each *Hin*dIII–*Nco*I fragment was excised and subcloned into pPGB II, giving rise to Sp1 binding site-replaced mutants, pB8-189(Sp1X) for Sp1 binding site X (X = A, B and C). The *Sph*I–*Hin*dIII fragment of pB8-189(Sp1A) was subcloned into pKF19k, and then subjected to site-directed mutagenesis using the mutagenic primer for Sp1 binding site C as described above. Then the *Hin*dIII-*Nco*I fragment was excised and subcloned into pPGBII, giving rise to the Sp1 binding site-replaced mutant, pB8-189(Sp1AC), for Sp1 binding sites A and C. All plasmids were verified by restriction analysis and sequencing.

For the ST6GalNAc IV promoter, Sp1 binding site–replaced mutants, pR1-1232(Sp1A′), pR1-1232(Sp1B′), pR1-1232(Sp1C′), and pR1-1232(Sp1A′C′), were constructed as

TABLE II. **Exon/intron junctions of the ST6GalNAc III and IV genes.** The nucleotide sequences at the intron (lowercase letters) and exon (uppercase letters) junctions are shown. The derived amino acid sequence is shown below the nucleotide sequence. The same amino acid residues between the ST6GalNAc III and IV genes are underlined. Exons are numbered from the 5′ end. The exon sizes are indicated in bp. The numbering starts at the adenosine of the initiator methionine as +1.

Exon (bp)		Splice donor	Intron		Splice acceptor
ST6GalNAc III					
			6		7
1	89	TGC ATC CTC	AAG gtaacagctc	tgttttgcag	AGG AAG CCC GTG
		Cys Ile Leu	Lys		Arg Lys Pro Val
			71		72
2	195	AGG ACC CAA	GAG gtaagacctg	tcttttcag	CCT TTG CAA CTG
		Arg Thr Gln	Glu		Pro Leu Gln Leu
			207		209
3	410	ACT GGA AAG	GAC AGgtgagtcc	ttcctccagA	GTC CAG TCT GGC
		Thr Gly Lys	Asp		Val Gln Ser Gly
			243		245
4	108	GAA ACC TAC	TGC AAgtaagatc	ctctttcagG	ACA GAA GGG TAT
		Glu Thr Tyr	Cys		Thr Glu Gly Tyr
ST6GalNAc IV					
1	139	TCC GCT CGT	TCG gttagcgccc	cttgcctcag	TTT CTC TCA TAT
			4		5
2	101	ATG AAG GCC	CCG gtaagtgaca	tctccctcag	GGC CGC CTT CTG
		Met Lys Ala	Pro		Gly Arg Leu Leu
			66		67
3	186	CCA GAC GGG	AAG gtgagtcagc	ttctctgtag	CCT CTT ATC CGA
		Pro Asp Gly	Lys		Pro Leu Ile Arg
			203		205
4	413	ACA GGC AAG	AAC CGgtgagctg	cctcctcagG	AGA CAA TCA GGC
		Thr Gly Lys	Asn		Arg Gln Ser Gly
			239		241
5	108	GAT AGT TAC	TGC AGgttagacc	tcctaacagC	GAG AAG AGT CCC
		Asp Ser Tyr	Cys		Glu Lys Ser Pro

follows. A 1.9 kb *Sph*I–*Hin*dIII fragment of pR1-1232 was subcloned into pKF18k (Takara), and then subjected to site-directed mutagenesis using mutagenic primers, R1-Sp1X′ for Sp1 binding site X′ (X = A, B, and C), with a Mutan-Super Express Km kit. From these mutagenized plasmids, each *Hin*dIII–*Nco*I fragment was excised and subcloned into pPGB II, giving rise to Sp1 binding site-replaced mutants, pR1-1232(Sp1A′) for Sp1 binding site A′, pR1-1232(Sp1B′) for Sp1 binding site B′, and pR1-1232-(Sp1C′) for Sp1 binding site C′, respectively. The *Sph*I–*Hin*dIII fragments of pR1-1232(Sp1A′), pR1-1232(Sp1B′), and pR1-1232(Sp1C′) were each subcloned into pKF18k, and then subjected to site-directed mutagenesis as described above to construct Sp1 binding site double-replaced mutants. After mutagenesis, each *Hin*dIII–*Nco*I fragment from these plasmids was excised and subcloned into pPG-BII, giving rise to the Sp1 binding site double-replaced mutants, pR1-1232(Sp1A′B′), pR1-1232(Sp1A′C′), and pR1-1232(Sp1B′C′) for Sp1 binding sites A′ and B′, A′ and C′, and B′ and C′, respectively. The *Sph*I–*Hin*dIII fragment of pR1-1232(Sp1A′B′) was subcloned into pKF18k, and then subjected to site-directed mutagenesis as described above to construct an Sp1 binding site triple-replaced mutant. After mutagenesis, the *Hin*dIII–*Nco*I fragment of the mutagenized plasmid was excised and subcloned into pPG-BII, giving rise to the Sp1 binding site triple-replaced mutant, pR1-1232(Sp1A′B′C′). All plasmids were verified by restriction analysis and sequencing.

RESULTS

Isolation of Mouse ST6GalNAc III and IV Genomic Clones—Screening of an NIH3T3 cosmid genomic library with full length mouse ST6GalNAc III cDNA resulted in the isolation of four independent, non-overlapping cosmid clones (Fig. 1A). The location of the ST6GalNAc III exons was determined by hybridization and PCR. Sequencing was performed to determine the exact sizes of the exons and exon-intron junctions (Table II). The ST6GalNAc III gene was found to be divided into 5 exons, ranging from 89 to 3080 bp, spanning over 120 kb of genomic DNA.

We also screened a C57BL/6 mouse cosmid genomic library with full length ST6GalNAc IV cDNA, and cloned three independent overlapping clones (Fig. 1A). Analysis of these clones revealed that the ST6GalNAc IV gene is divided into 6 exons, ranging from 101 to 2683 bp, spanning about 12 kb of genomic DNA. Although the entire genome size of the ST6GalNAc III gene is 10 times or more larger than that of the ST6GalNAc IV gene, and the ST6-GalNAc IV gene has an extra exon, the ST6GalNAc III and IV genes have very similar genomic structures. The sequences of the exon-intron splice junctions of both genes obey the GT-AG rule (*17*) (Table II). The splice junctions of the ST6GalNAc III gene in exons 1–2 and 2–3 are between codons, and those in exons 3–4 and 4–5 occur after the second nucleotide of the amino acid codon. Similarly, the splice junctions of the ST6GalNAc IV gene in exons 2-3 and 3-4 are between codons, and those in exons 4–5 and 5–6 are

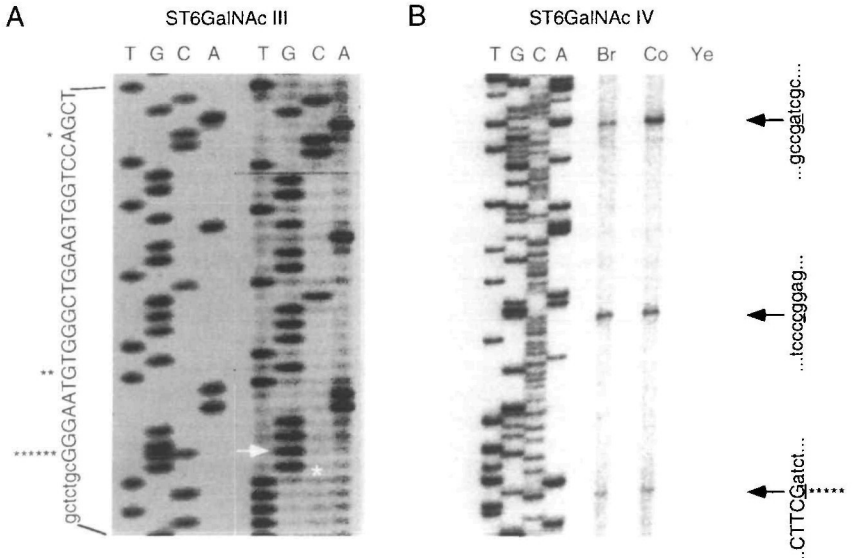

Fig. 2. **Analysis of the transcription initiation sites of the ST6GalNAc III and IV genes.** (A) 5′-RACE PCR analysis of ST6GalNAc III mRNA. PCR products were subcloned into pUC119 and then subjected to DNA sequence analysis. The white arrow indicates the major cDNA end generated on RACE-PCR. The white asterisk shows the nucleotide that may be the result of the terminal transferase activity of reverse transcriptase. The asterisks on the nucleotide sequence indicate the obtained cDNA ends of the RACE-PCR clones. (B) Primer extension analysis of ST6GalNAc IV mRNA. Primer extended products of brain mRNA (Br), colon mRNA (Co), and yeast tRNA (Ye) were run on a sequencing gel along with a corresponding sequence ladder. Arrows and asterisks indicate the identified transcription initiation sites by primer extension and 5′-RACE PCR, respectively.

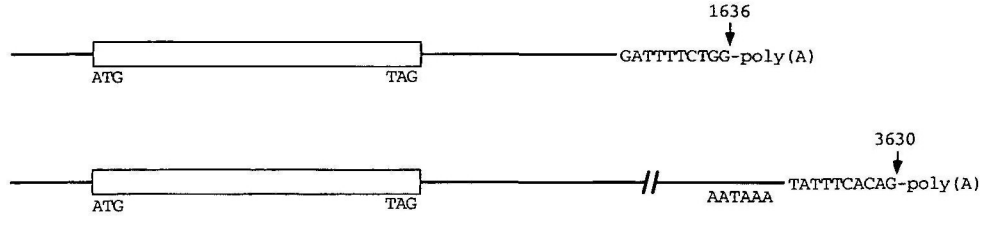

Fig. 3. **Analysis of the 3′-end of the ST6GalNAc IV transcripts.** 3′-RACE PCR was performed as described under "MATERIALS AND METHODS." The identified structures of the two transcripts are shown schematically.

after the second nucleotide of the amino acid codon. Comparison of the corresponding exons between the ST6GalNAc III and IV genes showed they share significant homology (Fig. 1B). For the ST6GalNAc III gene, exon 1 contains the 5′-untranslated region and a part of the cytoplasmic domain. Exon 2 encodes the hydrophobic signal anchor sequence and the stem domain. Exons 3–5 encode the putative active domain of the enzyme. Exon 5 contains a trans-

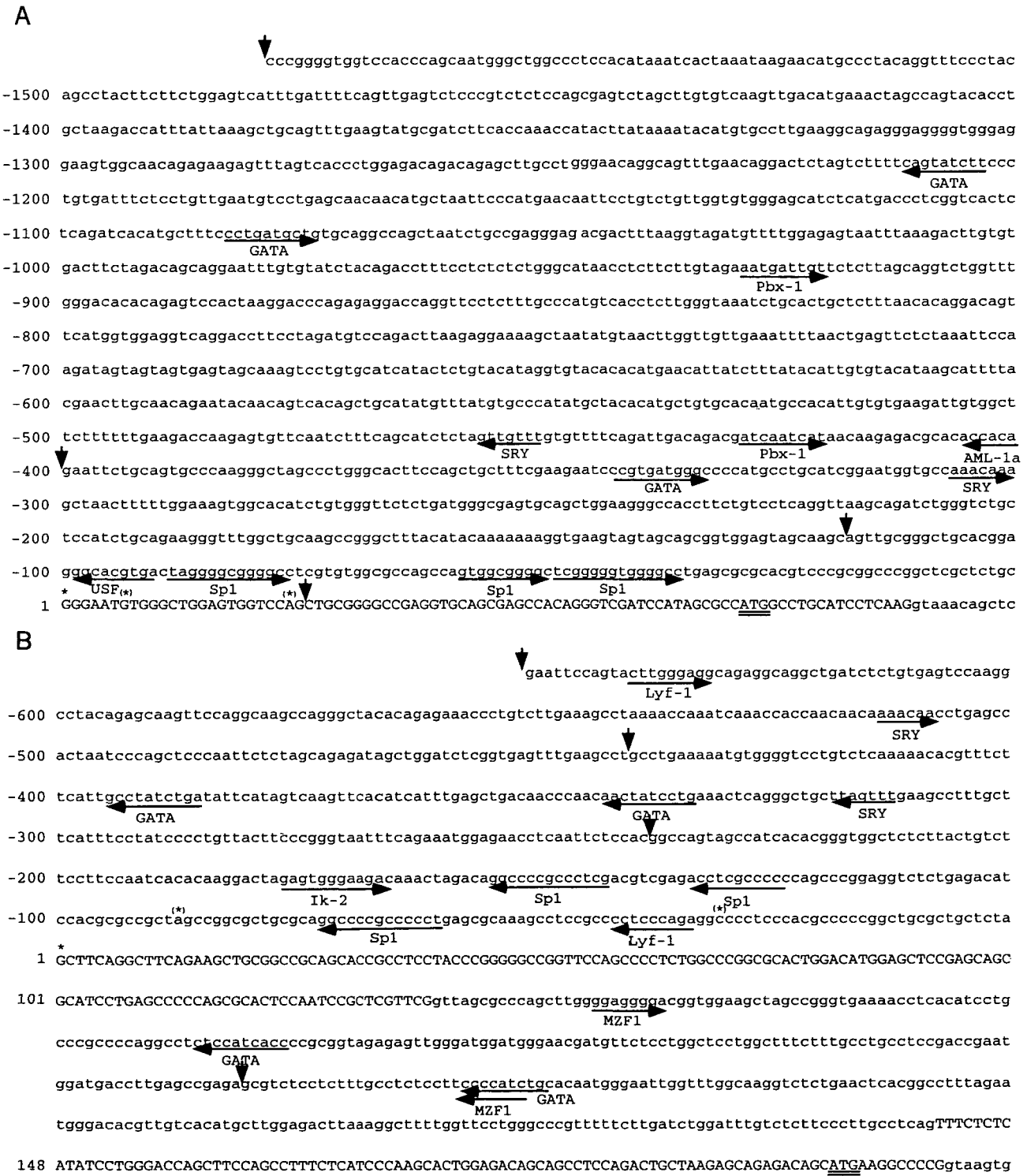

Fig. 4. **Nucleotide sequence of the 5′-flanking regions of the ST6GalNAc III (A) and IV (B) genes.** The exon sequences are shown in capital letters, while those of the untranscribed regions are given in lowercase letters. The transcription initiation sites are indicated by asterisks. The numbering of the nucleotides begins with the major transcription initiation site determined on 5′-RACE PCR being taken as +1. The translation initiation codon is double underlined. The consensus binding sequences of some transcription factors are shown by arrows. For the detection of promoter activity, the start point of each construction is indicated by an arrowhead.

lation termination codon and a long 3′-untranslated region. The same can be said for the corresponding exons of the ST6GalNAc IV gene.

Mapping of the Transcription Initiation Sites—The major transcription initiation site of the ST6GalNAc III gene was determined by 5′-RACE as described previously (*9*). Sequencing of 5′-RACE PCR clones revealed that most of the transcription initiation sites map at guanosine 71 upstream from the adenosine at the translational initiation site, which is designated as nucleotide +1 (Fig. 2A).

The major transcription start site of the ST6GalNAc IV gene was also determined by 5′-RACE PCR with RNA recovered from mouse brain or colon. Sequencing of 5′-RACE PCR clones revealed that most of the transcription initiation sites map at guanosine 228.

We also performed primer extension analysis determine the transcription initiation sites of the ST6GalNAc IV gene (Fig. 2B). The primer extension product terminated at guanosine 228 upstream from the adenosine of the translational initiation site, which coincides with the transcription initiation site determined by 5′-RACE PCR. However, two extra transcription initiation sites were also identified, one at adenosine 316 and the other at cytidine 259. The reason we could not detect the two sites on 5′-RACE PCR may be that some secondary structures in the upstream region prevent the extension.

Analysis of the Heterogeneity of ST6GalNAc IV Transcripts—In our previous study, we found that there are at least three species of transcripts for the ST6GalNAc IV gene [1.6–1.9, 2.0–2.2, and 3.6–3.7 kb (*9*, *10*)]. We examined whether or not the differences between these mRNA isoforms are the result of alternative splicing by means of PCR and Northern blot analysis. The results of PCR amplification of ST6GalNAc IV cDNA and Northern blot analysis using different positions of the cDNA sequence as probes suggested that the three different sized transcripts encode the same translation product, but have untranslated regions of different lengths. As described above, there are at least three different transcription initiation sites for ST6GalNAc IV transcripts, but they are relatively close to one another. So we performed 3′-RACE PCR to investigate the diversity of the 3′-untranslated region. Sequence analysis of the 3′-RACE PCR products revealed at least two polyadenylation sites in the 3′-untranslated region. The first polyadenylation site is located at nucleotide position 1636 (Fig. 3), but no typical polyadenylation signal (AATAAA) was found for this polyadenylation site. The second polyadenylation site is located at nucleotide position 3630 (Fig. 3), and a typical polyadenylation signal was found for this site (nucleotide positions 3612 to 3617). The first and second polyadenylation sites correspond to the 1.6–1.9 and 3.6–3.7 kb transcripts, respectively. We could not identify the polyadenylation site for the 2.0–2.2 kb transcript for unknown reasons. It may be that the secondary structures of this mRNA prevents the extension reaction on 3′-RACE PCR. On the other hand, the expression of the ST6GalNAc III gene is too low to detect by Northern hybridization, so we could not determine the exact number of ST6GalNAc III transcripts (*9*).

Promoter Analysis of the ST6GalNAc III and IV Genes, and Demonstration of Promoter Activity—Analysis of the sequence immediately upstream of the transcription initiation site revealed that the ST6GalNAc III and IV promoters contain no canonical TATA or CCAAT box, but each contains three putative Sp1 sites, (G/T)GGGCGG(G/A)(G/A)(C/A), at nucleotide positions –87 (putative Sp1 binding

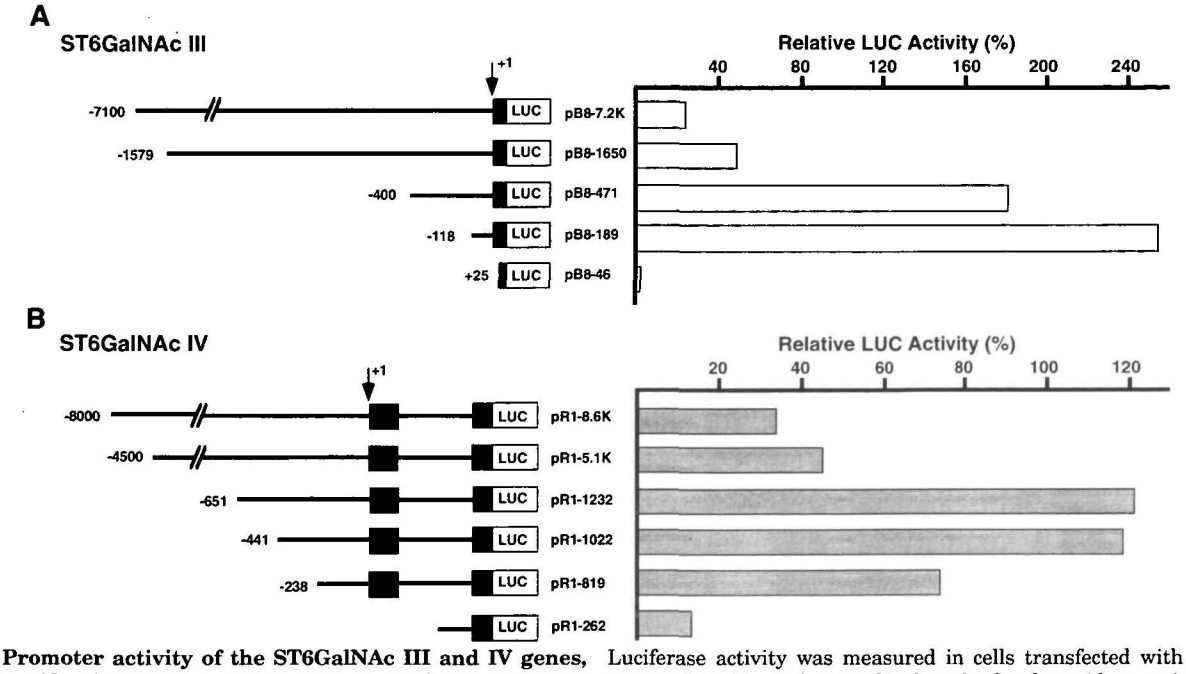

Fig. 5. **Promoter activity of the ST6GalNAc III and IV genes, and identification of the regulatory regions.** Schematic representation of DNA constructs containing various lengths of the promoter linked to the luciferase gene (pPGBII). Each DNA fragment subcloned into the luciferase reporter plasmid is defined by its position in the promoter relative to the transcription initiation site (+1). Luciferase activity was measured in cells transfected with the reporter plasmids, and normalized to the β-galactosidase activity of a cotransfected internal control plasmid, pSRβ-Gal, and expressed as a percentage of the SV40 promoter activity. (A) The ST6GalNAc III promoter activity in P19 cells. (B) The ST6GalNAc IV promoter activity in NIH3T3 cells.

site A, matching 10 to 10), –59 (putative Sp1 binding site B, matching 9 to 10), and –46 (putative Sp1 binding site C, matching 9 to 10) for the ST6GalNAc III promoter (Fig. 4A), and at nucleotide positions –155 (putative Sp1 binding site A′, matching 9 to 10), –134 (putativeSp1 binding site B′, matching 8 to 10), and –73 (putative Sp1 binding site C′, matching 10 to 10) for the ST6GalNAc IV promoter (Fig. 4B). The Sp1 binding sequence is considered to be typical of a housekeeping gene promoter. There are also some putative elements for binding transcription factors, GATA (*18*), Pbx-1 (*19*), SRY (*20*), AML-1a (*21*), USF (*22*), LyF-1 (*23*), Ik-2 (*24*), and MZF1 (*25*), in these promoters, but no similarities were observed between these two promoters (Fig. 4).

To characterize the regions regulating the transcription activity of the ST6GalNAc III and IV genes, chimeric reporter plasmids encoding the luciferase gene and promoter regions were constructed. The resultant chimeric constructs were transfected into a ST6GalNAc III–expressing cell line, P19, for analysis of the ST6GalNAc III promoter activity, and a ST6GalNAc IV–expressing cell line, NIH3T3 for analysis of the ST6GalNAc IV promoter activity. As a negative control, the plasmid pPGBII, containing the promoterless luciferase gene, was transfected into parallel cultures. The luciferase activity due to each luciferase reporter plasmid was normalized for β-galactosidase activity by cotransfecting an internal control plasmid, pSRβ-Gal, carrying the β-galactosidase gene under the control of the SRα promoter,

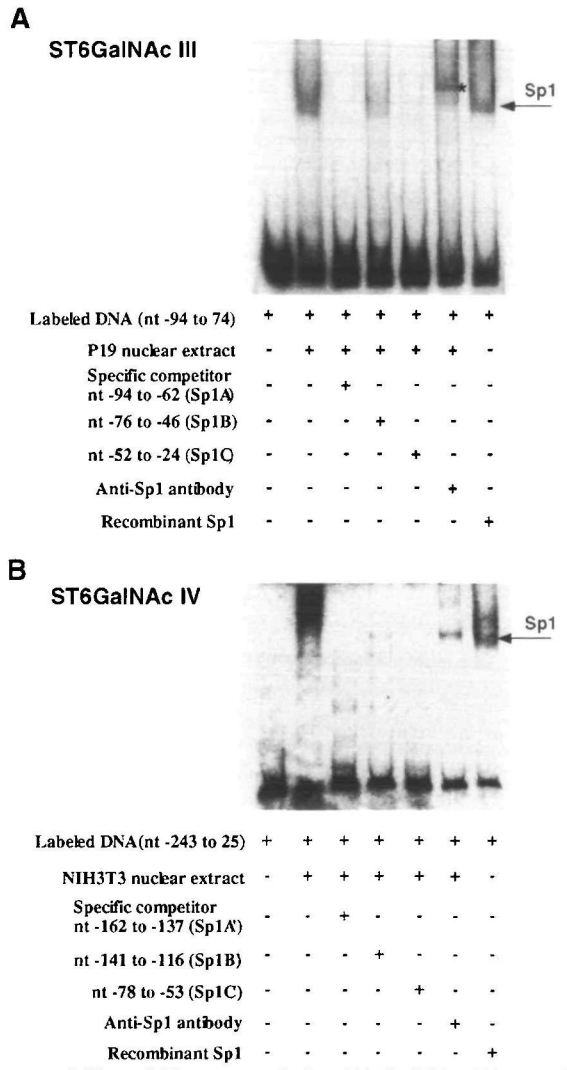

Fig. 6. **Mobility shift assay of the ST6GalNAc III proximal promoter region with a nuclear extract of P19 cells (A), and the ST6GalNAc IV proximal promoter region with a nuclear extract of NIH3T3 cells (B).** (A) The 5′-end labeled DNA fragment of the ST6GalNAc III proximal promoter region comprising nucleotides –94 to 74 (lane 1) was incubated with a nuclear extract of P19 cells either alone (lane 2) or with 25 times the amount of the non-labeled specific competitor (synthetic DNA fragment from –94 to –62 for lane 3; synthetic DNA fragment from –76 to –46 for lane 4; and synthetic DNA fragment from –52 to –24 for lane 5), and the anti-Sp1 antibodies (lane 6), and then subjected to the mobility shift assay. Lane 7 shows the results of a mobility shift assay involving 0.4 footprinting units of recombinant Sp1 instead of the nuclear extract of P19 cells. The asterisk indicates the supershifted band. (B) The 5′-end labeled DNA fragment of the ST6GalNAc IV proximal promoter region comprising nucleotides –243 to 25 (lane 1) was incubated with a nuclear extract of NIH3T3 cells either alone (lane 2) or with 25 times the amount of the non-labeled specific competitor (synthetic DNA fragment from –162 to –137 for lane 3; synthetic DNA fragment from –141 to –116 for lane 4; and synthetic DNA fragment from –78 to –53 for lane 5), and the anti-Sp1 antibodies (lane 6), and then subjected to the mobility shift assay. Lane 7 shows the results of a mobility shift assay involving 0.4 footprinting units of recombinant Sp1 instead of the nuclear extract of NIH3T3 cells.

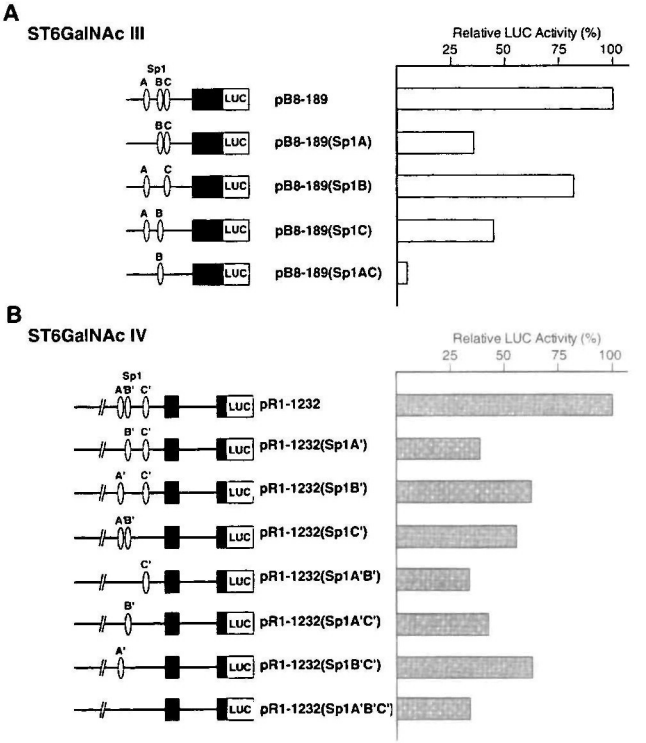

Fig. 7. **Mutational analysis of the ST6GalNAc III (A) and IV (B) proximal promoter regions.** Schematic representation of pB8-189 and pR1-1232 mutants with replacement mutations of the Sp1 binding sites in the ST6GalNAc III and IV promoters, respectively, and their promoter activities. Each of the relative promoter activities was measured as the luciferase activity in P19 cells for pB8-189 derivatives and in NIH3T3 cells for pR1-1232 derivatives, normalized to the β-galactosidase activity of a cotransfected internal control plasmid, pSRβ-Gal. The values are presented as percentages of the promoter activity due to pB8-189 and pR1-1232.

and expressed as a percentage of the SV40 promoter activity.

Among the ST6GalNAc III promoter constructs, those other than pPGBII and pB8-46 exhibited more or less functional promoter activity in P19 cells (Fig. 5A). Deletion of the upstream sequences increased the promoter activity, and a high level of transcriptional activity comparable to that of the SV40 promoter was observed with the pB8-471 and pB8-189 constructs in P19 cells. This suggests that some negatively regulating elements are included in the upstream region from –7.1 to –1.6 kb. Further deletion of the promoter to position +25 drastically reduced the promoter activity, indicating that the first 189 bp upstream sequence from the translational initiation codon contains the minimum promoter for expression by P19 cells. Among the ST6GalNAc IV promoter constructs, those other than pPGBII exhibited more or less functional promoter activity in NIH3T3 cells (Fig. 5B). Deletion of the upstream sequences increased the promoter activity, and a high level of transcriptional activity, comparable to that of the SV40 promoter, was observed with the pR1-1232 and pR1-1022 constructs in NIH3T3 cells. This suggests that some negatively regulating elements are included in the upstream region from –8.0 to –0.7 kb. Further deletion of the promoter gradually reduced the promoter activity, and deletion to the position in the first intron greatly reduced the promoter activity, indicating that the first 441 bp upstream sequence from the translational initiation codon contains the minimum promoter for expression by NIH3T3 cells.

Involvement of Sp1 in the Transcription of the ST6GalNAc III and IV Genes—There are three putative Sp1 binding sites for each of the proximal promoter regions of the ST6GalNAc III and IV genes. To determine whether or not these putative Sp1 binding sites are recognized by Sp1 and involved in the transcriptional regulation of these genes, we performed a mobility shift assay experiment.

For the ST6GalNAc III promoter, the *Pma*CI–*Nco*I fragment (nucleotide positions –94 to 74), which contains three putative Sp1 binding sites, was used in the mobility shift experiment. The recombinant Sp1 bound to this fragment (Fig. 6A, lane 7). A corresponding band to that observed in the presence of recombinant Sp1 appeared in the presence of the nuclear protein extract of P19 cells (lane 2). This shifted band super-shifted upon the addition of anti-Sp1 polyclonal antibodies (lane 6), indicating that Sp1 in the nuclear extract of P19 cells recognizes some of the putative Sp1 binding sites in this fragment. The shifted band was abolished by the addition of non-labeled specific competitors (lanes 3 and 5, synthetic DNA fragments from nucleotide positions –94 to –62 for putative Sp1 binding site A, and –52 to –24 for putative Sp1 binding site C), but not by the addition of a non-labeled specific competitor for putative Sp1 binding site B (lane 4, nucleotide positions –76 to –46). These results indicate that putative Sp1 binding sites A and C are involved in the transcription of ST6GalNAc III mRNA, but that the putative binding site B is not.

To clarify the involvement of these putative Sp1 binding sites in transcription, we constructed Sp1 binding site-replaced mutants of pB8-189 and analyzed their promoter activities in P19 cells. The Sp1 binding site B–replaced mutant, pB8-189(Sp1B), had little effect on the promoter activity (Fig. 7A). In contrast, the Sp1 binding site A–replaced mutant, pB8-189(Sp1A), and the Sp1 binding site C–replaced mutant, pB8-189(Sp1C), caused a reduction in the promoter activity to 35.5 and 44.1%, respectively, as compared with the wild-type construct (Fig. 7A). These results correspond to those of the mobility shift experiments. Moreover, the Sp1 binding site A and C double–replaced mutant, pB8-189(Sp1AC), caused a drastic reduction in the promoter activity to 4.5% that of the wild-type construct, sug-

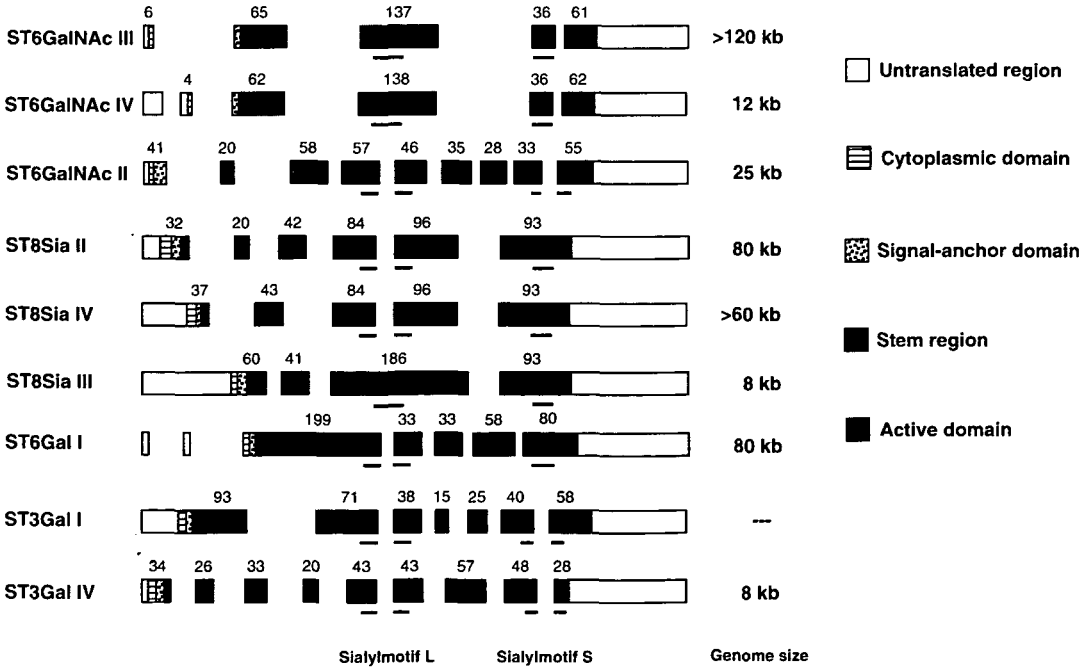

Fig. 8. **Genomic organization of sialyltransferase genes.** The intron–exon structures of nine sialyltransferase genes are shown. The protein domain structure is represented schematically by a rectangle, which is subdivided to show the major structural elements of the protein. Sialyl motifs L and S are underlined.

gesting that Sp1 binding sites A and C are synergistically involved in the transcription of ST6GalNAc III mRNA.

For the ST6GalNAc IV promoter, the *Xho*I–*Eco*52I fragment (nucleotide positions –243 to 25) from pR1-1232, which contains three putative Sp1 binding sites, was used in the mobility shift experiment. The recombinant Sp1 bound to this fragment (Fig. 6B, lane 7). This band is broad, probably because multiple binding of Sp1 occurred. A corresponding broad band to that observed in the presence of recombinant Sp1 appeared in the presence of the nuclear protein extract of NIH3T3 cells (lane 2). Most of this shifted band disappeared upon the addition of anti-Sp1 polyclonal antibodies (lane 6), indicating that Sp1 in the nuclear extract of NIH3T3 cells recognizes some putative Sp1 binding sites in this fragment. The shifted band was abolished by the addition of non-labeled specific competitors (lanes 3, 4, and 5, synthetic DNA fragments from nucleotide positions –162 to –137 for putative Sp1 binding site A′, –141 to –116 for putative Sp1 binding site B′, and –78 to –53 for putative Sp1 binding site C′), but minor bands remained, suggesting that some nuclear proteins other than Sp1 bind specifically to this fragment. These results indicate that all of these putative Sp1 binding sites are involved in the transcription of ST6GalNAc IV mRNA.

To clarify the involvement of these putative Sp1 binding sites in transcription, we constructed Sp1 binding site–replaced mutants of pR1-1232 and analyzed their promoter activities in NIH3T3 cells. All of the Sp1 binding site–replaced mutants caused significant reduction in the promoter activity to 34.1 to 64.0%, as compared with the wild-type construct (Fig. 7B). These results correspond to those of the mobility shift experiments. However, binding site double-replaced mutants did not cause a drastic reduction in the promoter activity, as in the case of pB8-189(Sp1AC) for the ST6GalNAc III promoter, suggesting that these Sp1 binding sites are independently involved in the transcription of ST6GalNAc IV mRNA. In addition, the binding site triple-replaced mutant also did not cause a drastic reduction in the promoter activity. This suggests that there are other transcription factors, which may be related to minor bands seen in the mobility shift experiment, involved in the basic transcription of ST6GalNAc IV mRNA.

DISCUSSION

In this study, we determined the genomic organization of the mouse ST6GalNAc III and IV genes, and characterized their promoter regions by means of transient transfection assays with a luciferase-reporter system and gel mobility shift assays using nuclear extracts of cultured cells.

So far, the genomic organization of several other sialyltransferase genes has been reported (*8*, *15*, *16*, *26–30*). Among them, the genomic structures of the polysialic acid synthase (ST8Sia II and IV) genes are fairly similar to each other (*16*, *26*) (Fig. 8). In this study, we have shown that the ST6GalNAc III and IV genes represent another case of genomic structural resemblance. The sizes of the exons of the ST6GalNAc III gene are almost the same as those of the corresponding exons of the ST6GalNAc IV gene, and the exon–intron boundaries of these genes are also similar to each other. According to the sequence similarity and substrate specificity, ST6GalNAc III and IV belong to the same subfamily, and it has been suggested that they have quite different domain structures from those of other sialyltransferases (*9*). These findings indicate that the ST6GalNAc III and IV genes arose from a common ancestral gene through gene duplication. It is interesting that although their genomic structures are similar, the overall genome size of the ST6GalNAc III gene is ten or more times greater than that of the ST6GalNAc IV gene.

In spite of their high structural similarity, the expression patterns of the ST6GalNAc III and IV genes are quite different. The expression level of the ST6GalNAc III gene in adult mouse is very low, and is found mainly in brain, lung and heart, while that of the ST6GalNAc IV gene is relatively high, and is found mainly in brain, colon, lung, heart, thymus and spleen (*9*). The different expression patterns of the two genes can be explained by the functions of their structurally different promoters. Indeed, the nucleotide sequences of the 5′-flanking regions of the two genes show no significant similarity, except that they contain no TATA or CCAAT box, but have some binding sites for Sp1 (Fig. 4).

In order to identify the regulatory regions of these promoters, we performed a promoter assay experiment using a luciferase-reporter system. The results suggested that there are some negative regulatory regions in the upstream region of each promoter. We also identified the regions containing the minimum promoter. There are Sp1 binding sites in these regions, and so we examined the involvement of Sp1 in the transcription of these genes. The results suggested that the two Sp1 binding sites are synergistically involved in the transcriptional regulation of the ST6GalNAc III gene in P19 cells, while three Sp1 binding sites are independently involved in the transcriptional regulation of ST6GalNAc IV mRNA in NIH3T3 cells. There are at least three transcription initiation sites for the ST6GalNAc IV gene. The independency of each Sp1 site may be related to the multiplicity of the transcription initiation sites of this gene. The expression level of the ST6GalNAc IV gene is higher than that of the ST6GalNAc III gene (*9*). The difference between the basic transcriptional regulation of these genes by Sp1 may also be related to the expression levels of these genes.

We have identified and characterized the essential promoter regions of six mouse sialyltransferase genes, ST6GalNAc II, III, and IV, and ST8Sia II, III, and IV (*8*, *15*, *16*, *26*). The 5′-flanking regions of all these genes have at least one Sp1 binding motif. Mobility shift assay and site-directed mutagenesis of the putative Sp1 binding sites revealed that Sp1 is involved in the transcriptional regulation of the ST6GalNAc II gene (Footnote 6), and the ST8Sia II (Footnote 6) and IV (*16*) genes. A ubiquitous transcription factor, NF-Y, is also involved in the transcriptional regulation of the ST8Sia IV gene (*16*). Sp1 is thought to be a ubiquitous transcription factor associated with the transcriptional regulation of housekeeping genes (*31–33*). Identification of essential transcription factors will be useful for understanding the basic transcription mechanism of sialyltransferase genes. However, we have not yet identified transcription factors other than Sp1 involved in the specific promoter activities in the examined cells. Some other transcription factors may be involved in these specific promoter activities and the tissue-specific expression of the ST6GalNAc III and IV genes. Identification of such transcription factors may facilitate understanding of the different expression patterns of the ST6GalNAc III and IV genes, and also

the mechanisms for tissue- and stage-specific expression. Work along these lines is currently in progress. The availability of five members of the ST6GalNAc-family, together with the stage-specific control sequence and transgenic animal technique, will provide further information to help elucidate of the biological functions of sialylglycoconjugates through alteration of the glycoconjugate expression pattern during development.

We wish to thank Dr. Yoshitaka Nagai, Director of the Glycobiology Research Group, and Dr. Tomoya Ogawa, Coordinator of the Group, Frontier Research Program of the Institute of Physical and Chemical Research (RIKEN), for their support in this work.

REFERENCES

1. Svennerholm, L. (1964) The gangliosides. *J. Lipid. Res.* **5**, 145–155
2. Tsuji, S., Datta, A.K., and Paulson, J.C. (1996) Systematic nomenclature for sialyltransferases. *Glycobiology* **6**(7), v–vii
3. Tsuji, S. (1996) Molecular cloning and functional analysis of sialyltransferases. *J. Biochem.* **120**, 1–13
4. Tsuji, S. (1999) Molecular cloning and characterization of sialyltransferases in *Sialobiology and Other Novel Forms of Glycosylation* (Inoue, Y., Lee Y.C., and Troy, F.A., eds) pp. 145–154, Gakushin Publishing Company, Osaka
5. Kurosawa, N., Hamamoto, T., Lee, Y.-C., Nakaoka, T., Kojima, N., and Tsuji, S. (1994) Molecular cloning and expression of GalNAcα2,6-sialyltransferase. *J. Biol. Chem.* **269**, 1402–1409
6. Kurosawa, N., Kojima, N., Inoue, M., Hamamoto, T., and Tsuji, S. (1994) Cloning and expression of Galβ1,3GalNAc-specific GalNAcα2,6-sialyltransferase. *J. Biol. Chem.* **269**, 19048–19053
7. Sjoberg, E.R., Kitagawa, H., Glushka, J., van Halbeek, H., and Paulson, J.C. (1996) Molecular cloning of a developmentally regulated *N*-acetylgalactosamine α2,6-sialyltransferase specific for sialylated glycoconjugates. *J. Biol. Chem.* **271**, 7450–7459
8. Kurosawa, N., Inoue, M., Yoshida, Y., and Tsuji, S. (1996) Molecular cloning and genomic analysis of mouse Galβ1, 3GalNAc-specific GalNAc α2,6-sialyltransferase. *J. Biol. Chem.* **271**, 15109–15116
9. Lee, Y.-C., Kaufmann, M., Kitazume-Kawaguchi, S., Kono, M., Takashima, S., Kurosawa, N., Liu, H., Pircher, H., and Tsuji, S. (1999) NeuAcα2,3Galβ1,3GalNAc GalNAcα2,6-sialyltransferase family, ST6GalNAc III and IV. *J. Biol. Chem.* **274**, 11958–11967
10. Kaufmann, M., Blaser, C., Takashima, S., Schwartz-Albiez, R., Tsuji, S., and Pircher, H. (1999) Identification of an α2,6-sialyltransferase induced early after lymphocyte activation. *Int. Immunol.* **11**, 731–738
11. Okajima, T., Fukumoto, S., Ito, H., Kiso, M., Hirabayashi, Y., Urano, T., Furukawa, K., and Furukawa, K. (1999) Molecular cloning of brain-specific GD1α synthase (ST6GalNAc V) containing CAG/glutamine repeats. *J. Biol. Chem.* **274**, 30557–30562
12. Ikehara, Y., Shimizu, N., Kono, M., Nishihara, S., Nakanishi, H., Kitamura, T., Narimatsu, H., Tsuji, S., and Tatematsu, M. (1999) *FEBS Lett.* **463**, 92–96
13. Ishikawa, D., Taki, T., Nakajima, M., and Handa, S. (1995) Ganglioside GD1α as an adhesion molecule of murine metastatic tumor cells. *Glycoconjugate J.* **12**, 523
14. Furuya, S., Irie, F., Hashikawa, T., Nakazawa, K., Kozaki, A., Hasegawa, A., Sudo, K., and Hirabayashi, Y. (1994) Ganglioside GD1α in cerebellar Purkinje cells. Its specific absence in mouse mutants with Purkinje cell abnormality and altered immunoreactivity in response to conjunctive stimuli causing long-term desensitization. *J. Biol. Chem.* **269**, 32418–32425
15. Yoshida, Y., Kurosawa, N., Kanematsu, T., Taguchi, A., Arita, M., Kojima, N., and Tsuji, S. (1996) Unique genomic structure and expression of the mouse alpha 2,8-sialyltransferase (ST8Sia III) gene. *Glycobiology* **6**, 573–580
16. Takashima, S., Yoshida, Y., Kanematsu, T., Kojima, N., and Tsuji, S. (1998) Genomic structure and promoter activity of the mouse polysialic acid synthase (mST8Sia IV/PST) gene. *J. Biol. Chem.* **273**, 7675–7683
17. Shapiro, M.B. and Senapathy, P. (1987) RNA splice junctions of different classes of eukaryotes: sequence statistics and functional implications in gene expression. *Nucleic Acids Res.* **15**, 7155–7174
18. Merika, M. and Orkin, S.H. (1993) DNA-binding specificity of GATA family transcription factors. *Mol. Cell. Biol.* **13**, 3999–4010
19. Van Duk, M.A., Voorhoeve, P.M., and Murre, C. (1993) Pbx1 is converted into a transcriptional activator upon acquiring the N-terminal region of E2A in pre-B-cell acute lymphoblastoid leukemia. *Proc. Natl. Acad. Sci. USA* **90**, 6061–6065
20. Pontiggia, A., Rimini, R., Harley, V.R., Goodfellow, P.N., Lovell-Badge, R., and Bianchi, M.E. (1994) Sex-reversing mutations affect the architecture of SRY-DNA complexes. *EMBO J.* **13**, 6115–6124
21. Meyers, S., Downing, J.R., and Hiebert, S.W. (1993) Identification of AML-1 and the (8;21) translocation protein (AML-1/ETO) as sequence-specific DNA-binding proteins: the runt homology domain is required for DNA binding and protein-protein interactions. *Mol. Cell. Biol.* **13**, 6336–6345
22. Read, M.L., Clark, A.R., and Docherty, K. (1993) The helix-loop-helix transcription factor USF (upstream stimulating factor) binds to a regulatory sequence of the human insulin gene enhancer. *Biochem. J.* **295**, 233–237
23. Lo, K., Landau, N.R., and Smale, S.T. (1991) LyF-1, a transcriptional regulator that interacts with a novel class of promoters for lymphocyte-specific genes. *Mol. Cell. Biol.* **11**, 5229–5243
24. Molnár, Á. and Georgopoulos, K. (1994). The Ikaros gene encodes a family of functionally diverse zinc finger DNA-binding proteins. *Mol. Cell. Biol.* **14**, 8292–8303
25. Morris, J.F., Hromas, R., and Rauscher III, F.J. (1994) Characterization of the DNA-binding properties of the myeloid zinc finger protein MZF1: two independent DNA-binding domains recognize two DNA consensus sequences with a common G-rich core. *Mol. Cell. Biol.* **14**, 1786–1795
26. Yoshida, Y., Kurosawa, N., Kanematsu, T., Kojima, N., and Tsuji, S. (1996) Genomic structure and promoter activity of the mouse polysialic acid synthase gene (mST8Sia II). Brain-specific expression from a TATA-less GC-rich sequence. *J. Biol. Chem.* **271**, 30167–30173
27. Svensson, E.C., Soreghan, B., and Paulson, J.C. (1990) Organization of the β-galactoside α2,6-sialyltransferase gene. Evidence for the transcriptional regulation of terminal glycosylation. *J. Biol. Chem.* **265**, 20863–20868
28. Wang, X., O'Hanlon, T.P., Young, R.F., and Lau, J.T. (1990) Rat β-galactoside α2,6-sialyltransferase genomic organization: alternate promoters direct the synthesis of liver and kidney transcripts. *Glycobiology* **1**, 25–31
29. Chang, M.L., Eddy, R.L., Shows, T.B., and Lau, J.T. (1995) Three genes that encode human β-galactoside α2,3-sialyltransferases. Structural analysis and chromosomal mapping studies. *Glycobiology* **5**, 319–325
30. Kitagawa, H., Mattei, M.-G., and Paulson, J.C. (1996) Genomic organization and chromosomal mapping of the Galβ1,3GalNAc/Galβ1,4GlcNAc α2,3-sialyltransferase. *J. Biol. Chem.* **271**, 931–938
31. Kadonaga, J.T., Jones, K.A., and Tijan, R. (1986) Promoter specific activation of RNA polymerase II transcription by Sp1. *Trends Biochem. Sci.* **11**, 20–23
32. Saffer, J.D., Jackson, S.P., and Thurston, S.J. (1990) SV40 stimulates expression of the transacting factor Sp1 at the mRNA level. *Genes Dev.* **4**, 659–666
33. Saffer, J.D., Jackson, S.P., and Annarella, M.B. (1991) Developmental expression of Sp1 in the mouse. *Mol. Cell. Biol.* **11**, 2189–2199